A numerical approach for estimating the aerodynamic characteristics of a two bladed vertical Darrieus wind turbine

Ervin Amet, Christian Pellone, Thierry Maître

Scientific Bulletin of the
Politehnica University of Timisoara
Transactions on Mechanics
Special issue

2nd Workshop on
Vortex Dominated Flows
Bucharest, Romania
June 30 – July 1, 2006

A NUMERICAL APPROACH FOR ESTIMATING THE AERODYNAMIC CHARACTERISTICS OF A 2 BLADED VERTICAL DARRIEUS WIND TURBINE

Ervin AMET, Phd. Student*
Laboratory of Geophysical and Industrial Fluid Flows
Institut National Polytechnique de Grenoble
Technical University of Civil Engineering of Bucharest

Christian PELLONE, Scientist Researcher CNRS
Laboratory of Geophysical and Industrial Fluid Flows
Institut National Polytechnique de Grenoble

Thierry MAITRE, Assoc. Prof. INPG
Laboratory of Geophysical and Industrial Fluid Flows
Institut National Polytechnique de Grenoble

**Corresponding author*: Laboratoire des Ecoulements Géophysiques et Industriels, BP53, 38041, Grenoble, France
Email: Ervin.Amet@hmg.inpg.fr

ABSTRACT

This paper presents the results of a numerical investigation on the turbulent flow on a 2D Darrieus turbine. This flow is particularly complex for two reasons: as the turbines rotates, the incidence angle and the blade's Reynolds number changes, involving strong unsteady effects in the flow field. The most important of them consists in a continuous dynamic separation of the flow, which influences the performance of the turbine. The numerical model used to describe the flow is an explicit RANS K-omega code (academic Turbflow™ software). The use of a block - structured mesh allows high order numerical schemes involving low numerical dissipation. The final objective of this work is to model precisely the flow on the two-NACA airfoils Darrieus turbine studied experimentally by Laneville and Vittecoq [4]. In particular, an improvement of the dynamic stall modeling, compared with a previous numerical study [Ploesteanu and Maitre, 2003], [2] is expected. Firstly, the paper presents the main features of the flow in a Darrieus turbine. Secondly it focus on the dynamic stall phenomenon and presents the main results obtained in the aformentionned previous study. Finally the first results obtained with the present approach are commented. Because the rotating test cases are at present in progress, this paper presents partial results for non rotating configurations corresponding to three angular positions of the turbine. These configurations allow to discuss the starting capability of the Darrieus turbine and highlight the promising ability of the modeling to take into account large stalled region.

KEYWORDS

Darrieus turbine, Reduced frequency, Dynamic stall, Stall vortices, Lift and drag hysteresis

NOMENCLATURE

C_0 [m] airfoil chord
R [m] radius of the rotor
H [m] height of the rotor
D [m] diameter
S [m^2] cross-sectional area of the turbine
L [N] lift force
D [N] drag force
F [N] aerodynamic force
F_n [N] normal force
F_t [N] tangential force
θ [rad] azimuth angle of the blade
α_0 [°] offset pitch angle of the blade
α_{SS} [°] static stall angle
α [°] blade incidence angle with relative velocity
CL [-] lift coefficient
CD [-] drag coefficient
CP [-] power coefficient
CM [-] torque coefficient
CN [-] normal coefficient

CT [-] tangential coefficient

C_p [-] pressure coefficient

ω [rpm] angular speed of the rotor

λ [-] tip speed ratio

W [m/s] relative velocity

U_∞ [m/s] undisturbed airspeed upstream

P_m [W] power received on the rotor's shaft

σ [-] solidity

P [W] power of the unconstrained uniform flow

n [-] number of blades

ν [m^2/s] air cinematic viscosity

k [-] reduced frequency

1. INTRODUCTION

This paper presents the results of a series of numerical tests on a vertical axis wind turbine with 2 straight NACA 0018 blades. The behaviour of this type of turbine is an essential issue of the HARVEST Project of LEGI Laboratory in France. The objective of this project is to develop a suitable technology for a hydroelectric marine or river power farm using vertical axis marine turbines. For air applications, this kind of turbine suffer of vibrations, due to large variation of the torque within one revolution, that can lead to its destruction. This drawback explain the lesser use of this technology compared with horizontal axis turbines. For marine and river applications, the decrease of the inflow velocity (2m/s compared to 10m/s in air) lead to a decrease of rotational speed and centrifugal forces on the blades. This effect allow the use of particular blade shape (that differ of the classical troposkian shape in air) that reduce greatly the variation of the torque in a revolution and consequently the vibrations, like Gorlov [1] or Achard [2] (figure 1). Moreover, these new shape allow the self starting of the turbine. The two main advantages of vertical axis turbines remain: insensitivity to the inflow direction, possibility to stack the turbines on a same axis equipped with one generator only. This gathering of turbines is called a tower.

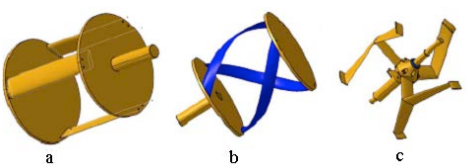

Figure 1. View of three typical turbines:
a - Darrieus; b - Gorlov; c - Achard

Although Darrieus wind turbine is relatively a simple device to construct, the aerodynamics of the blades is very complex. The turbine's aerodynamics is affected by a group of complex and coupled phenomenon's: high unsteady flows, interaction between blades, dynamic stall, low and varying Reynolds numbers, fluid – structure coupling, 3D effects and the possibility of cavitation at low pressure level. The attendant dynamic forces and moments exhibit large amount of hysteresis with respect to the incidence angle, especially if α oscillates around a mean value α_0, that is of the order of the static stall angle α_{SS}. [3] To take into account the flow's complexity, a simplified approach is necessary in the first step. A 2D model of the Darrieus turbine was chosen for comparing the results for the drag and lift coefficients with the experimental data available in Laneville and Vittecoq [4] paper. In a previous study Cristina Ploesteanu [5] obtained, using the commercial code Fluent, a good description of the first stage of the vortex detachment from blades phenomenon. However, the typical load hysteresis undergo by the blades was not obtained. It was shown that the life time of the shed vortices was to short in the calculation to influence the load of the foil from witch they detached. To avoid this difficulty, it was decided to use a dedicated academic code, Turbflow[1], allowing high order numerical schemes. The benefit expected is a gain of precision but at the price of less numerical stability and more effort for the multi-block structured grid generation. The equations solved by Turbflow are the full 3D, unsteady, compressible RANS equations with low Mach preconditioning for incompressible flows. The flux separation is based on a MUSCL formulation with finites volumes [6]. The turbulence is described either by a LES algorithm or by a two model equation k-ω Wilcox or k-ω Kok, using Runge–Kutta time integration. The latter is used in this study.

2. GENERAL HYDRODYNAMICS

The forces acting on a blade are summarized in figure.2. We can decompose the forces either by respect with the fluid speed direction (into lift and drag), or with respect to the blade (normal and tangential force). When the turbine rotates, with the angular speed ω, the airfoil experiences a variation

[1] **Developped by Ecole Centrale de Lyon and FLUOREM**

of the incidence angle α according to a sinusoidal law for a high tip speed ratio that distorts to a saw tooth shape for a tip speed ratio equal to unity. [4].

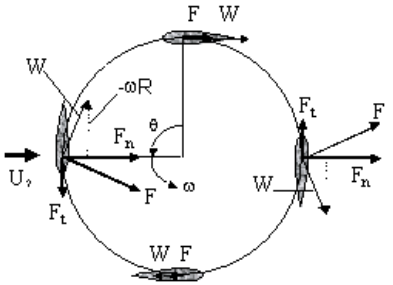

Figure 2. Forces and velocities components on the foil

The speed ratio is defined as the ratio between the linear velocity and the flow speed, as follows:

$$\lambda=\frac{\omega R}{U_\infty} \tag{1}$$

It should be noted that the local incidence angle α varies according to the following law:

$$\alpha=tan^{-1}\left(\frac{sin\theta}{\lambda+cos\theta}\right) \tag{2}$$

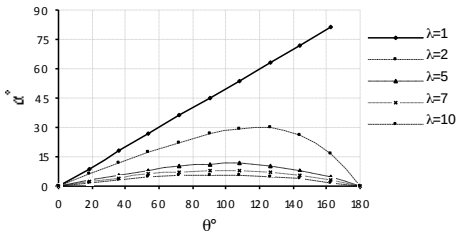

Figure 3. Incidence angle with respect to the azimutal angle

For $\lambda=2$, the incidence angle on the blades varies continuously during a revolution from 0° for θ=0° and 180° to around 30° for θ=120° and 240. When λ increases, the maximum incidence angle decreases and occurs near θ=90° and 270°. The tangential component F_t of the aerodynamic force F gives the torque to the turbine (figure 2). Globally it can be said that the upstream and downstream part of the disc give a positive torque thought the top and bottom give a negative one. Consequently, the blades receive, during one revolution, a cyclic fluid force and although the appearance of the dynamic stall acts positively on the power generation of the turbine [7], the presence of stall vortices produces problems, such as aero elastic vibrations and noises from the blades and the fatigue of the blade by the unsteady forces [8].

The important characteristics for a water turbine are the blade shape, the number of blades and the solidity. The solidity is defined as the ratio of the entire blade surface to the swept area of the blade. In our case, for a blade chord length C_0, n blades, radius R, the solidity S is defined as:

$$\sigma=\frac{nC_0H}{S} \tag{3}$$[2]

The blade Reynolds number in our case is expressed as follows:

$$Re=\frac{\omega RC_0}{\nu} \tag{4}$$

For a typical Darrieus turbine, this blade's Reynolds number is moderate, (around $5\cdot10^4$ in air and in water), leading to unsteady laminar turbulent transition during the revolution.

To characterize the wind or water turbine performance, two main parameters are used: the power coefficient and the torque coefficient.

The power coefficient is defined as the ratio of the power received on the rotor's shaft and the

$$CP=\frac{P_m}{\frac{1}{2}\rho SU_\infty^3} \tag{5}$$

kinetic power of the upstream flow.

Fig. 4, shows a typical efficiency curve of a Darrieus turbine performance.

[2] **Other equations (depending on authors) for solidity:** $\frac{nC_0}{R}$; $\frac{nC_0}{2\pi R}$

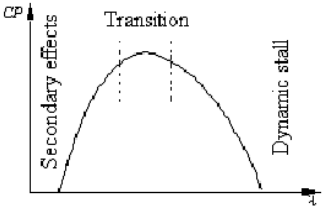

Figure 4. The power coefficient variation with the tip speed ratio (Paraschivoiu , 2002 [10])

Usually, the tip speed ratio range is from 1 to 10 and the maximum power coefficient varies from 0.2 to 0.4 depending of the kind of turbine (Darrieus, helical, troposkian) of its size and of the fluid (air or water). For water application, the best power coefficient obtained up to now corresponds to the Gorlov helical turbine: around 35% [4]. The curve can be splinted into 3 distinct zones: the dynamic stall regime, where the solidity, the airfoil lift and the dynamic stall are important; the secondary effects regime, [9], where the shaft, the flanges, the added mass and the viscosity friction are to be considered and the transition zone where the maximum power occurs. This last zone corresponds to different tip speed ratio range by considering different typical parameter of the turbine like solidity for example. [5,10]

3. THE DYNAMIC STALL

It is essential to be able to predict the complex flow on a Darrieus turbine, not only to determine the average power recovered, but also to anticipate the cyclic loads that stress the blades and induce fatigue. All the structures securing the marine current turbines are the most likely to be weakened by the vibrations. It should also be noted that the wake downstream of a turbine must be accurately known, as it potentially decrease the inflow of the downstream towers of the farm and increase the risk of vibrations of these devices.

The flow through a straight Darrieus turbine was visualized at the University of Sherbrooke [Brochier *and al.*, 1986] (figure 5).The presence of two main contra-rotating vortices a and b passing through the machine and continuing downstream was noted. The basic characteristic of these vortices is that they remain close to the blade that generated them. There is therefore a strong coupling between the vortices and flow around the blade, which causes a high-lift effect that is advantageous to the performance of the machine. These dynamic separation mechanisms are similar to those observed in helicopter rotors [McCroskey, 1981] [3].

In his paper, McCroskey stated that the dynamic stall for an oscillating blade, with an offset pitch angle α_0, an amplitude of α_{max}, following a sinusoidal law, is strongly influenced by the parameter reduced frequency k. The reduced frequency is [4]:

$$k=C_0\cdot\left(d\alpha/dt\right)/(\omega R\times 2\alpha_{max}) \quad (6)$$

For a Darrieus turbine, the reduced frequency k, equivalent to a helicopter's blade is:

$$k=C_0/2R(\lambda-1)tan^{-1}(\lambda^2-1)^{-1/2}=A(\lambda)\frac{c}{R} \quad (7)$$

If k is small, the flow will have the time to stabilize, it is almost quasi-static. If $k>0.05$, the turbine will be experiencing dynamic stall every time the incidence angle will exceeds the static stall angle α_{SS}.

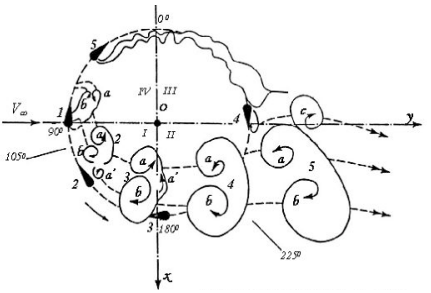

Figure 5. Stalled flow in a Darieus turbine, from [G. Brochier and al., 1986], [9]

The figure 6 presents the lift coefficient against the incidence angle during a revolution, for a speed ration λ= 2 corresponding to the strong stall region of the turbine. This figure highlights the difference between the large hysteresis loop given by the tested model (white square marks) and the small one given by the calculation (dark points marks). It is found that the 2 main contra-rotating vortices a and b are well predicted during the first stage of their development. However, their circulation decreases drastically during the ulterior stage corresponding to their convection inside the turbine. For this reason, the flow reattaches prematurely to the blade, leading to a quasi-static flow and consequently to the evanescence of the hysteresis loop.

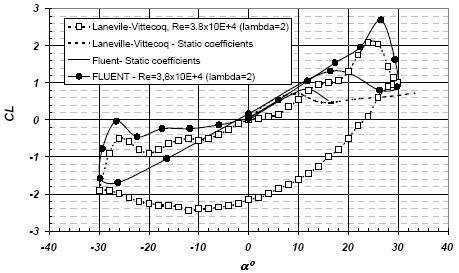

Figure 6. Lift coefficient versus incidence angle [5]

4. K ω TURBULENT MODEL

The k-ω Kok model, including the cross-diffusion term, are given by:

$$\frac{\partial \rho k}{\partial t}+\frac{\partial(\rho k u_j)}{\partial x_j}=P_k-\beta^*\rho\omega k+\frac{\partial}{\partial x_j}\left((\mu+\sigma_k\mu_t)\frac{\partial k}{\partial x_j}\right) \quad (8)$$

$$\frac{\partial \rho\omega}{\partial t}+\frac{\partial(\rho\omega u_j)}{\partial x_j}=P_\omega-\beta\rho\omega^2+\frac{\partial}{\partial x_j}\left((\mu+\sigma_\omega\mu_t)\frac{\partial \omega}{\partial x_j}\right)+C_{DIF} \quad (9)$$

with ρ the density, $\vec{u}$ the velocity vector, μ the molecular viscosity coefficient, k the turbulent kinetic energy, ω specific turbulent dissipation and $\mu_t=\rho k/\omega$ the eddy-viscosity coefficient.

The production and cross-diffusion terms are given by:

$$P_k=\tau_{ij}^R\frac{\partial u_j}{\partial x_i} \quad (10)$$

$$P_\omega=\frac{\alpha_\omega\omega}{k}P_k \quad (11)$$

$$C_{DIF}=\sigma_d\frac{\rho}{\omega}max\left\{\frac{\partial k}{\partial x_i},\frac{\partial \omega}{\partial x_i},0\right\}, \quad (12)$$

with τ^R the Reynolds stress tensor, $\overbrace{\sigma_d,\ \sigma_k,\ \sigma_\omega}^{TNT}$, β^*, β , α_ω are the closure coefficients.

The solutions of the standard Wilcox $k-\omega$ model are dependent on the free-stream values of the turbulence variables, even at low free-stream eddy-viscosity levels. When the so-called cross-diffusion term is included in the equation for ω (when positive), the $k-\omega$ model becomes formally equivalent to the $k-\varepsilon$ type models near free-stream edges of turbulent regions. This model, however, requires the wall distance to evaluate the blending function, thus loosing one of the advantages of the $k-\omega$ model. An alternative approach is to enforce the correct (large) value of ω at the boundary-layer edge. However, the large value of ω may have the undesired effect that laminar/turbulent transition is suppressed at specified transition lines [11]. In the $k-\omega$ Kok model, a new set of closure coefficients (TNT) has been chosen that should resolve the free-stream dependency for the model. In our case, $k-\omega$ Kok model uses the Runge–Kutta time integration, with local time stepping.

5. GEOMETRY AND GRID GENERATION

In order to reproduce Laneville and Vittecoq [3] experiment, a straight, two bladed Darrieus turbine is simulated, with $H=0.6m$, $R=0.3m$, $C_0=0.061m$, corresponding to a solidity of 0.02. The blade's shape is a symmetrical NACA 0018 foil type. As reported by [8, 10], for low tip speed ratio (2 *to* 4), the influence of the central shaft and flanges are neglected. The section area of the test section is $1.82\ m \times 1.82\ m$, with no corrections for the blockage effect. The offset pitch angle is $\alpha_0=0$. The chord is tangential to the 0.3 m diameter circle at the first quarter point of the chord. The inflow velocity is set equal to 4.71, corresponding to a blade Reynolds number of: $Re=3.8\cdot10^4$.

A multi block-structured mesh is used and the whole domain was meshed with the Fluent preprocessor Gambit and then divided in 28 structured blocks (figure 7). Then Each block is written separately in a PLOT3D ASCII format file, recognizable by the CFD solver Turbflow. The whole procedure is automated with different Fortran utility software developed in the laboratory. The simulation were carried out in an PVM multiprocessor environment at C.I.N.E.S.[3], FRANCE. C.I.N.E.S. offer to laboratories the opportunity to run their scientific codes in a parallel programming environment. The simulations were performed on a SGI ORIGIN 3800 platform, a parallel supercomputer with 512 processors R14000+/500 Mhz.

The total number of cells is 224498, giving an average cells block number varying from 2000 to 17000. To properly resolve the viscous affected region, a U shape mesh is used around the foils and y+ at the wall adjacent cell is chosen around 1, corresponding to a size of 25 μm (figure 6). Typically, for a test case using 30 processors, the

[3] **Centre Informatique National de l'Enseignement Supérieur**

actual computation time is 13.8 hours. The same calculation with one processor would lead to 10 times more computation time.

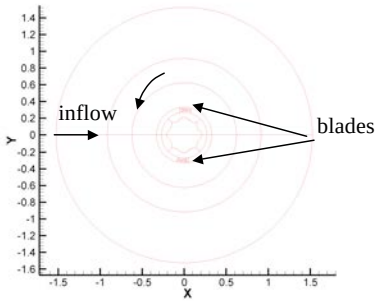

Figure 7. Block structured mesh

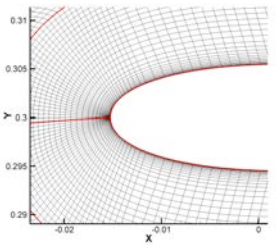

Figure 8. U mesh in the blade region

6. RESULTS

Because the rotating test cases are at present in progress, this paper presents partial results for non rotating configurations corresponding to three angular positions of the turbine: θ=0°, θ=45°, and θ=90° (figure 9). Figures 10, 11, 12 present respectively, the pressure coefficients on the foil 1, for θ=0° , θ=45°, θ=90°.

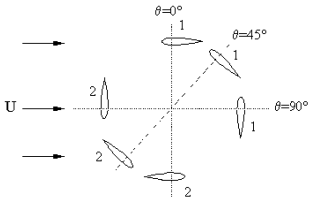

Figure 9. Angular position of the turbine

$$C_p = \frac{p - p_\infty}{0.5 \rho U_\infty^2} \quad (13)$$

The blue curve corresponds to the outer side of the foil. The minimum value of the pressure coefficient is about -0.5 compared to the theoretical value for an inviscid fluid of -0.62 [5,12]. This gap is due to viscous effects at low Reynolds number. The slight difference between the two sides values are due to the influence of the second foil on the first one, as shown in the figure 13. In the figure 11, the peak of low pressure coefficient near the leading edge is moderate (Cp_{min}=-3) because of the large re-circulating flow on the outer side (figure 16). In the figure 12, the same phenomenon is seen (Cp_{min}=-1.2), the center pressure is moving towards the trailing edge.

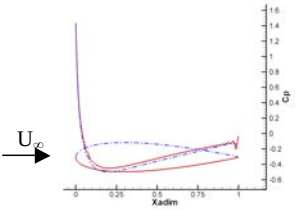

Figure 10. Pressure coefficient around the foil 2 for θ=0°

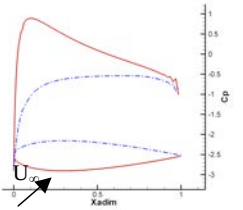

Figure 11. Pressure coefficient around the foil 2 for θ=45°

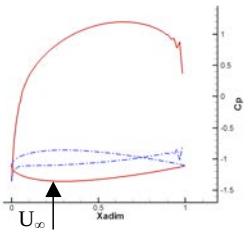

Figure 12. Pressure coefficient around the foil 2 for θ=90°

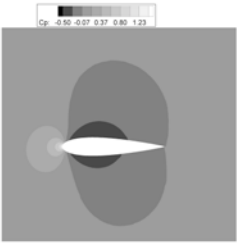

Figure 13. Contours of pressure for θ=0°

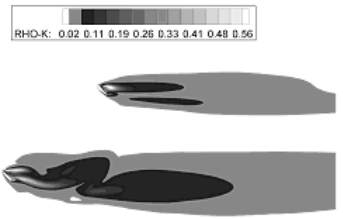

Figure 14. Turbulent kinetic energy contours for θ=45°

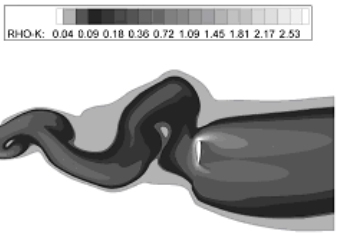

Figure 15. Turbulent kinetic energy contours for θ=90°

The figures 14 and 15 shows the turbulent kinetic energy k for θ=45° and θ=90°. In the first case, the wake asymmetry between the two foils is obvious. It is noticed that the fluid detachment at the trailing edge of foil 2, is stronger than that of foil 1. For θ=90°, the downstream (foil 1) is in the wake of the upstream foil (foil 2), as shown on the figures 18 and 19 . Consequently, the pressure on the foil 1 is affected by viscous effects (as discussed previously). The figure 16 is a zoom of the velocity field at the leading edge for θ=0°, the boundary layer is well captured.

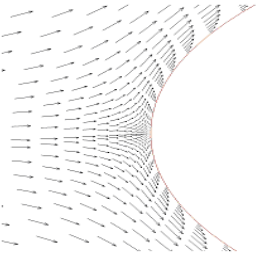

Figure 16. Velocity vectors for θ=0° near the leading edge

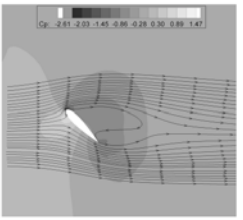

Figure 17. Streamlines vectors for θ=45° on foil 2

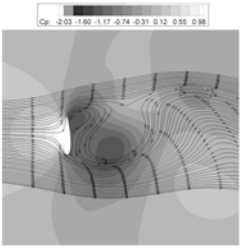

Figure 18. Pressure coefficients contours and streamlines for θ=90° on foil 2

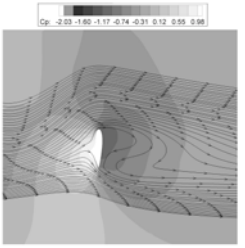

Figure 19. Pressure coefficients contours and streamlines for θ=90° on foil 1

7. CONCLUSION

Numerical simulations of a Darrieus turbine at low Reynolds number was performed using an academic RANS code Turbflow. The final objective of these simulations is to capture precisely the dynamic stall phenomenon. This present paper dealing with non-rotating configurations corresponds to the first step of the final objective. The block structured mesh allows high order numerical schemes. Moreover, the parallel capabilities of Turbflow allow fine grids that couldn't be used with mono-processor calculation. The global behavior of the flow is well described, particularly the vortex structures in the wake. Two objectives in the near future are to be reached. The first one concerns some validations of the present results with other numerical results in fixed configurations. The second one is the rotating calculation of the turbine. On the other hand, these results will be compared with experimental data obtained in LEGI's hydrodynamic tunnel and with other data obtained in the wind tunnel of UTCB.

REFERENCES

1. Gorlov A. M. The helical turbine and its applications for hydropower without dams. In: OCEANS 2003 Proceedings, Volume 4, 22-26 Sept. 2003 Page(s):1996 Vol.4
2. Maître T., Achard J.-L., Guittet L., Ploesteanu C. Marine turbine development: numerical and experimental investigations In: Scientific Bulletin of the "Politehnica" University of Timisoara, Tom 50(64), Issue 2, ISSN 1224-6077, pp. 59-66, 2005
3. W. J. McCroskey The Phenomenon of Dynamic Stall (Lecture notes) (march 1981) Presented to Von Kármán Institute Lecture Series, 9-13, Rhode-Saint-Genèse, Belgium
4. Laneville A. and Vittecoq P. Dynamic stall: The case of the vertical axis wind turbine. In: Journal of Solar Energy Engineering, Vol. 108, May 1986, pp 140-145
5. Cristina Ploesteanu Etude hydrodynamique d'un type d'hydraulienne à axe vertical pour les courants marins. Thèse de Doctorat de l'Institut National Polytechnique de Grenoble, décembre 2004
6. F.S. Lien and M.A. Leschziner Upstream monotonic interpolation for scalar transport with application to complex turbulent flows. In: International Journal for Numerical Methods in Fluids, 19 (6), 1994, pp 527-548
7. R. B. Noll, N. D. Ham Effects of dynamic stall on SWECS. In: Journal of Solar Energy Engineering, Vol. 104, 1982, pp 96-101
8. Nobuyuki Fujisawa, Satoshi Shibuya Observations of dynamic stall on Darrieus wind turbine blades. In: Journal of Wind Engineering and Industrial Aerodynamics 89, (2001), pp 201-214
9. Brochier G., Fraunié P., Béguier C., Paraschivoiu I. Water Channel Experiments of Dynamic Stall on Darrieus Wind Turbine Blades. In: Journal of propulsion, Vol 2 (5), Sept-Oct 1986, pp 445-449
10. Paraschivoiu I. Wind turbine design with emphasis on Darrieus concept. Polytechnic International Press, ISBN 2-553-00931-3, 2002
11. Kok J. C. Resolving the dependence on free-stream values for the k-omega turbulence model. In: AIAA Journal 37 (8), 2000, pp 1292-1295
12. Ira H. Abbott and Albert E. Von Doenhoff Theory of wing sections. Dover Publications, Inc. 1958